A Hierarchical Optimization-Based OMPC Algorithm for Power Sharing in Multi-module Fast EV Charging Systems

C G. Revathi[1], B.Padmavathi[2], G.Pradeep Naidu[3], S.Mastan Valli[4], S M Umair Arfath[5]

[1]Assistant Professor, Department of EEE, AITS, Kadapa

[2,3,4,5]Student (UG), Department of EEE, AITS, Kadapa

Abstract— This article introduces a novel Optimal Modular Power Coordination (OMPC) algorithm for multimodule, multiport Fast Electric Vehicle Chargers (FEVCs). The proposed algorithm addresses the critical challenge of coordinated power distribution at both the module and charger levels through a hierarchical optimization framework. At the upper layer, a mixed-integer optimization model determines the optimal number of active power electronic modules (PEMs), selects the most efficient modules for contribution, and governs inter-port PEM borrowing decisions. At the lower layer, a real-time convex optimization routine computes optimal power-sharing ratios among the selected PEMs while satisfying grid limitations, module constraints, and thermal operating conditions. A key contribution is the introduction of PEM borrowing, a new concept that enables flexible reallocation of module power across different charging ports, significantly enhancing the charging power range and enabling dynamic split dual-port operation. Comprehensive simulation and experimental case studies validate the proposed OMPC algorithm, demonstrating substantial improvements in charging flexibility, module utilization balance, and charging speed reliability. Results confirm that the OMPC approach effectively mitigates charging bottlenecks and enhances the overall performance of multimodule FEVC systems.

Keywords - Inter-port PEM Borrowing Decisions, Convex Optimization, Charging Bottlenecks

I. INTRODUCTION

The rapid proliferation of electric vehicles (EVs) has significantly increased the demand for high-power and flexible charging infrastructure. Fast Electric Vehicle Chargers (FEVCs) with multimodule and multiport architectures have emerged as a promising solution to meet these demands, offering high scalability, improved reliability, and fault tolerance [1], [2]. In such systems, effective power coordination is essential to ensure that available power is dynamically and efficiently distributed across multiple modules and charging ports.

Conventional power distribution strategies in multimodule FEVCs often rely on static allocation schemes or heuristic control methods. These approaches may result in suboptimal system performance, reduced charger utilization, and limited flexibility during simultaneous multi-EV charging events [3], [4]. Recent studies have explored advanced control strategies, including centralized and decentralized optimization-based methods, to improve power sharing performance while respecting grid constraints and module limits [5]–[7]. However, many of these techniques still struggle to adapt in real time to variations in charging demand, grid conditions, and thermal operational limits [8] – [12]. To overcome these limitations, this paper proposes a Hierarchical Optimization-Based Optimal Modular Power Coordination (OMPC) algorithm for multimodule, multiport FEVC systems. The proposed framework employs a two-layer hierarchical optimization structure. At the upper layer, a mixed-integer optimization model determines the optimal number of active power electronic modules (PEMs), selects the most efficient modules, and governs module borrowing across ports [13] – [15]. The PEM borrowing concept allows flexible inter-port power reallocation, expanding the feasible charging power range and enabling dynamic multi-vehicle charging. At the lower layer, a real-time convex optimization routine computes optimal power-sharing ratios among the selected PEMs while considering grid capacity, PEM operational constraints, and thermal limits. The remainder of this paper is organized as follows. Section II reviews related work on power coordination strategies for multimodule charging systems. Section III formulates the hierarchical optimization problem. Section IV details the proposed OMPC algorithm. Section V presents simulation and experimental results. Finally, Section VI concludes the paper and discusses future research directions.

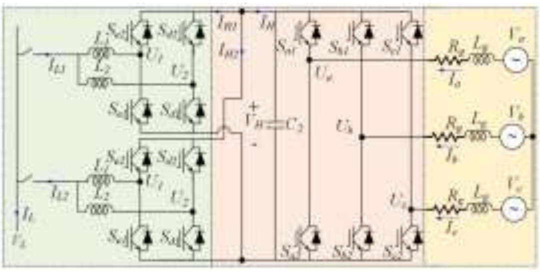

Fig. 1. Circuit diagram for PEM.

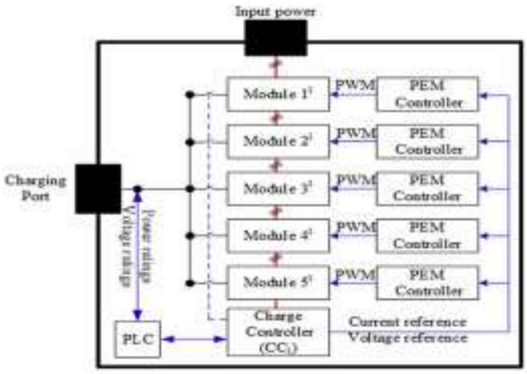

Fig. 2. Multimodule fast EV charger.

The contributions of this article are summarized as follows: 1) A novel energy management system is proposed for PEM-level and charger level of FEVCs. 2) A novel communication protocol is introduced for charge controllers' negotiation. 3) A new principle for PEM borrowing is proposed for both port level and charger level.

II. RELATED WORK

The rapid proliferation of electric vehicles (EVs) has led to extensive research on charging station architectures, power allocation mechanisms, and control strategies to improve charging performance and grid compatibility. Conventional multiport and multimodule fast EV chargers often rely on static or heuristic power distribution schemes, which can lead to inefficient utilization of available power resources and limited flexibility during simultaneous charging events [3]–[5]. Early work on multiport DC fast charging stations investigated optimal station design and power cap policies to balance cost and quality of service, highlighting the need for improved power allocation schemes under constrained grid capacity [turn1search3] and optimal planning of single-port versus multi-port infrastructures using mixed-integer programming. Dynamic power allocation strategies have been explored to better distribute limited converter capacity among charging ports in real time. For example, real-time power allocation policies based on stochastic or reinforcement learning frameworks have been proposed to adjust charging power dynamically according to queue conditions and grid limitations, enabling enhanced service levels in extreme charging scenarios [turn1search1]. Hierarchical approaches have also been considered in broader EV charging contexts — such as hierarchical dispatching strategies for integrating photovoltaic and storage systems with charging station operations [turn1search2] — and multi-level optimal charging management has been shown to improve energy utilization and reduce peak load stress in interoperable multiport systems with fleet charging hubs [turn1search5]. Several studies focus on multiport converter topologies and control rather than station-level power allocation. Multimodule DC–DC converter designs with differential power processing have been proposed to enable simultaneous charging of multiple EVs while reducing converter cost and improving efficiency, illustrating the importance of power sharing at the converter architecture level [turn0search7]. Similarly, hybrid multimodule converter topologies have been introduced to achieve high efficiency and power density through module grouping and uniform power sharing controls [turn0search4]. Recent literature has also started to address adaptive energy management techniques for multi-module and multi-port fast chargers. Notably, Sharida *et al.* propose an adaptive energy management technique that incorporates module selection, power-sharing computations, and inter-port power borrowing to support flexible charging operations, validated through simulation and experimental studies [turn0search1]. This work closely aligns with the core concepts targeted by the present Optimal Modular Power Coordination (OMPC) algorithm, demonstrating the relevance of advanced optimization for module selection and power distribution. Despite these advances, existing approaches often lack a unified hierarchical framework that simultaneously handles module activation decisions, optimal power allocation across modules, real-time responsiveness to grid and thermal constraints, and flexible inter-port reallocation (e.g., borrowing). The OMPC algorithm proposed in this paper builds on this body of work by introducing a mixed-integer upper layer for strategic module selection and a real-time lower layer for convex optimization-based power sharing, enabling enhanced charging flexibility and balanced module utilization across multi-EV charging scenarios.

III. POWER ELECTRONICS MODULES AND FEVC STRUCTURE

Each Power Electronics Module (PEM) in a Fast Electric Vehicle Charger (FEVC) consists of two cascaded converters: an AC–DC converter followed by a DC–DC converter, as shown. While these converters can be bidirectional, most commercially available FEVCs employ unidirectional converters due to cost constraints. Each PEM includes a dedicated communication interface and controller, which receives voltage and current reference signals to generate pulse-width modulation (PWM) control signals. Multiple PEMs can be connected in parallel, sharing a common AC input from the grid and a common DC output to the charging port. Each module is equipped with an output contactor or relay to connect or disconnect from the port. Dual-port chargers can be implemented using two sets of parallel modules. In conventional designs, power sharing between ports is not possible; to address this, a communication bus based on the CAN-Bus protocol links the PEMs with their respective charge controllers and enables inter-port coordination. In the case of PEM borrowing, modules associated with one port can temporarily provide power to another port. The borrowing port's charge controller then provides the reference and limit values, while the original port forwards these values to the borrowed modules.

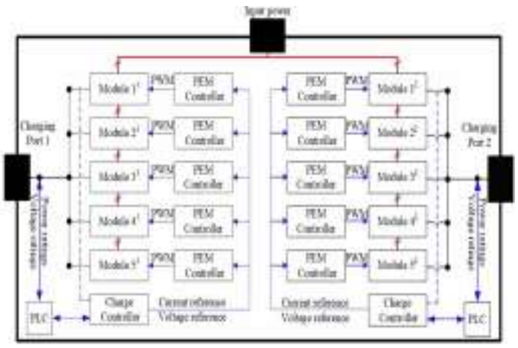

Fig. 3. Classical dual-port fast EV charger.

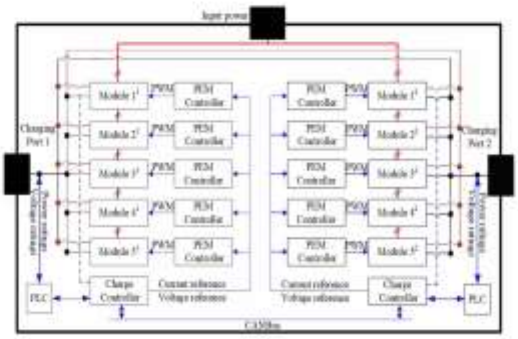

Fig. 4. Proposed dual-port fast EV charger structure.

IV. CONTROL TECHNIQUE FOR PEM-LEVEL

The AC–DC stage can be configured as either a single converter per DC–DC converter or multiple parallel converters feeding a common DC link. In this study, three AC–DC converters form a constant DC link voltage. One rectifier operates as the master to provide reference signals, while the others act as slaves. The AC–DC converters operate as active front-end rectifiers, with their output voltage denoted as $V_H$and current as I_H. The dynamic model of a three-phase rectifier is expressed as:

$$V_{abc} = L_g \frac{dI_{abc}}{dt} + R_g I_{abc} + U_{abc}$$

$$C\frac{dV_H}{dt} = \frac{3}{2}(V_d I_d + V_q I_q) - \frac{V_{dc}}{I_H}$$

where $L_g$and $R_g$are the input filter inductance and resistance, $V_{abc}$and $I_{abc}$are the grid voltage and current, and $U_{abc}$is the control signal. Voltage $V_H$is regulated indirectly through grid current control using standard controllers such as proportional-integral (PI) controllers or sliding mode controllers (SMC). In this study, a PI controller regulates the DC link voltage, while SMC is used for current regulation.

The DC–DC converters operate in two modes: battery-to-DC link (boost mode) and DC link-to-battery (buck mode). In the DC link-to-battery mode, the interleaved buck converter's dynamics are given by:

$$\frac{dI_{Ly}}{dt} = \frac{1}{L_y}(U_y - V_L - V_H - RI_{Ly})$$

$$\frac{dV_L}{dt} = \frac{1}{C}(I_{Ly} - \frac{V_H}{R_L})$$

The output current of each DC–DC converter is regulated using SMC as shown in Fig. 5.

V. CONTROL TECHNIQUE FOR CHARGE-CONTROLLER LEVEL

Each charge controller regulates the DC voltage at the charging port and coordinates all contributing PEMs. During the initial charging phase, the controller operates in constant current (CC) mode until the EV battery reaches 80% state of charge (SoC). Afterwards, the controller switches to constant voltage (CV) mode.

In CC mode, the total reference current is computed as:

$$I_{LT}^{CC} = \frac{P^*}{V_L}$$

where P^* is the reference charging power and V_L is the port voltage. If all PEMs have identical ratings, the current is shared equally; otherwise, each PEM contributes proportionally to its rated power:

$$I_{L,j}^{CC} = \frac{P_{R,j}}{\sum_{i=1}^{N_C} P_i^R} I_{LT}$$

During CV mode, the reference current is adjusted based on the voltage error $v_e = V_L - V_{L,ref}$, ensuring a smooth transition from CC to CV:

$$I_L^{CV} = K_p\, v_e$$

where the gain K_p is computed to match the current at the transition instant. In case of PEM borrowing, the borrowing charge controller computes the reference currents and forwards them to the lender controller, which relays the values to the respective PEMs.

VI. CONTROLLER METHODOLOGY

The proposed FEVC system employs a hierarchical control strategy consisting of two levels: PEM-level control and charge-controller-level coordination. This methodology ensures accurate voltage and current regulation, seamless transitions between charging modes, and flexible inter-port power sharing.

A. PEM-Level Control

Each PEM consists of an AC–DC converter followed by a DC–DC converter. The AC–DC converter maintains a constant DC link voltage V_H by regulating the input grid currents I_{abc} through a master-slave rectifier configuration. The dynamics of the three-phase rectifier are described as:

$$V_{abc} = L_g \frac{dI_{abc}}{dt} + R_g I_{abc} + U_{abc}$$

$$C\frac{dV_H}{dt} = \frac{3}{2}(V_d I_d + V_q I_q) - \frac{V_{dc}}{I_H}$$

where L_g and R_g are input filter parameters, V_{abc} and I_{abc} are the grid voltage and current, and U_{abc} is the control signal. A proportional-integral (PI) controller regulates the DC link voltage, while sliding mode control (SMC) regulates the DC current, ensuring robustness and fast dynamic response.

The DC–DC stage operates in two modes: battery-to-DC link (boost mode) and DC link-to-battery (buck mode). In buck mode, the interleaved DC–DC converter dynamics are:

$$\frac{dI_{Ly}}{dt} = \frac{1}{L_y}(U_y - V_L - V_H - RI_{Ly})$$

$$\frac{dV_L}{dt} = \frac{1}{C}\left(I_{Ly} - \frac{V_H}{R_L}\right)$$

The output current of each DC–DC converter is regulated using SMC to achieve fast response and minimize voltage overshoot. Fig. 5 illustrates the PEM-level control block diagram.

B. Charge-Controller-Level coordination

The charge controller manages all PEMs connected to a charging port and ensures seamless operation across **constant current (CC) and constant voltage (CV) modes**:

1. Constant Current Mode (CC):

At the beginning of the charging process, the controller computes the total reference current based on the EV's requested charging power $P^*$and port voltage V_L:

$$I_{LT}^{CC} = \frac{P^*}{V_L}$$

Each PEM contributes proportionally to its rated power $P_{R,j}$:

$$I_{L,j}^{CC} = \frac{P_{R,j}}{\sum_{i=1}^{N_C} P_i^R} I_{LT}$$

If all PEMs are identical, current is equally shared.

2. Constant Voltage Mode (CV):

When the EV battery reaches approximately 80% SoC, the controller switches to CV mode. The reference current is adjusted based on the voltage error $v_e = V_L - V_{L,ref}$:

$$I_L^{CV} = K_p\, v_e$$

The gain $K_p$is computed to ensure a smooth transition from CC to CV, preventing sudden current or voltage changes.

3. PEM Borrowing:

For dual-port operation, PEMs can be borrowed from one port to another. In this case, the borrowing controller computes the reference currents and forwards them to the lender controller, which relays the values to the respective PEMs. This enables flexible inter-port power allocation without violating module or port constraints.

C. Hierarchical Implementation

The hierarchical methodology allows separation of fast local regulation (PEM-level) and strategic power allocation (charge-controller-level). This structure ensures:

- Accurate DC link voltage and current control at the module level.
- Seamless CC–CV transitions at the port level.
- Dynamic and flexible distribution of power among modules and ports.

Scalable implementation for multiport, multimodule FEVC systems

VI. Case Studies

To validate the proposed PEM borrowing technique, two case studies are considered using multimodule, dual-port FEVCs. Each module has a rated power of 30 kW, and each port contains five PEMs unless otherwise specified.

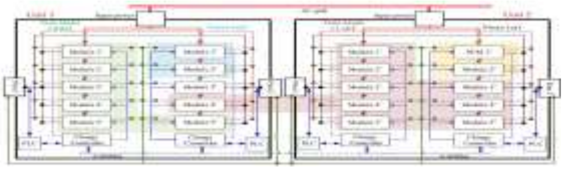

Fig. 5. Case study: PEMs borrowing between different charging units.

A. Case 1: Intra-Unit PEM Borrowing

In the first scenario, a dual-port charger has five PEMs per port, giving a total available power of 150 kW per port. A Nissan Leaf requiring 50 kW is connected to port 1, while a Tesla Model 3 Rear-Wheel Drive requiring 170 kW is connected to port 2. In conventional chargers, port 2 can provide a maximum of 150 kW, limiting the Tesla Model 3 to less than its nominal charge power. By adopting the proposed PEM borrowing technique, port 1 operates with only two PEMs, leaving three PEMs idle. Upon receiving a borrowing request from port 2, port 1 assigns one PEM to port 2, as illustrated in Fig. 6. Consequently:

- Port 1 uses two modules and keeps two modules idle.
- Port 2 has six modules in total (five original + one borrowed), supplying 180 kW.

As a result, both EVs can be charged at their nominal power without overloading any module or port.

B. Case 2: Inter-Unit PEM Borrowing

In the second scenario, a Nissan Leaf (50 kW) is connected to port 1 of another charger, requiring two PEMs, leaving three modules idle. A Tesla Model 3 Long Range and Performance (LARP) requires 250 kW, exceeding the power available in the five-module port 2. Without PEM borrowing, both EVs cannot be charged simultaneously at nominal power, increasing total charging time.

The proposed method resolves this as follows:

1. Feed the lower-power EV (port 1) and determine the number of idle PEMs.
2. Compute the total available power at the station, considering idle modules from port 2.
3. Borrow all idle PEMs from port 1.
4. If additional power is required, borrow PEMs from other charging units.

Assuming another unit (unit 1) is operating under the conditions in Case 1, it has two idle PEMs. These modules can be assigned to port 2 of unit 2. After borrowing:

- Port 2 of unit 2 has nine PEMs in total: five original, three borrowed from its own port 1, and one borrowed from unit 1 port 1.
- Total power available is 270 kW, sufficient to meet the Tesla Model 3 LARP charging requirement.

This case demonstrates the scalability and flexibility of the proposed PEM borrowing strategy across multiple charging units, ensuring optimal utilization of all available modules.

Algorithm 1: Module Selection Algorithm (OMPC-Inspired)

Procedure: SELECT_MODULES ()

1. Get EV-side requirements

Obtain demand $D$and requested EV power P_{EV}.

2. Get charger-side parameters

Obtain module power capacities P_{PEMs}, energy vector E, availability vector A, number of ports N_{port}, number of units N_{unit}, total number of modules C_{all}, and the target port port and unit unit.

3. Define decision variables

Define vector $\mathbf{m}$, consisting of C_{all}linear programming decision variables.

4. Define priority weights

Set weight vector $\mathbf{w} = [1, 10, 100]$.

i. Construct weighted energy cost vector

For each module $i \in \{1, \dots, C_{all}\}$:

- If module $i$belongs to the same port and the same unit:
  $$E_{tmp}(i) = w_1 \cdot E_i$$
- Else if module $i$belongs to the same unit but a different port:
  $$E_{tmp}(i) = w_2 \cdot E_i$$
- Otherwise:
  $$E_{tmp}(i) = w_3 \cdot E_i$$

ii. Case 1: Modules from the same port and same unit

- Construct availability vector A_{tmp}such that:

$A_{tmp}(i) = A_i$if module $i$is in the same port and same unit

$A_{tmp}(i) = 0$otherwise

- Solve the linear program using $\mathbf{m}$, E_{tmp}, and A_{tmp}
- If a feasible solution is found, return the set:
  $$\{ i \mid m_i > 0 \}$$

iii. Case 2: Modules from the same unit (different ports)

➢ Construct availability vector A_{tmp}such that:

$A_{tmp}(i) = A_i$if module $i$is in the same unit

$A_{tmp}(i) = 0$otherwise

- Solve the linear program using **m**, E_{tmp}, and A_{tmp}
- If a feasible solution is found, return the set:

$$\{ i \mid m_i > 0 \}$$

iv. Case 3: All available modules

- Solve the linear program using **m**, E_{tmp}, and A
- Return the set:

$$\{ i \mid m_i > 0 \}$$

End Procedure

OMPC-Inspired Module Selection Algorithm

1. Problem Definition

Consider a modular EV charger consisting of C_{all}power electronic modules (PEMs). Each module $i \in \{1,2,\dots,C_{all}\}$is characterized by:

- Available power capacity: P_i
- Energy cost (or degradation index): E_i
- Availability indicator: $A_i \in \{0,1\}$
- Port index: N_i^{port}
- Unit index: N_i^{unit}

The EV requests a charging power P_{EV}.

2. Decision Variables

Define binary selection variables:

$$m_i = \begin{cases} 1, & \text{if module } i \text{ is selected} \\ 0, & \text{otherwise} \end{cases}$$

Let:

$$\mathbf{m} = [m_1, m_2, \dots, m_{C_{all}}]^T$$

3. Objective Function (Weighted Energy Minimization)

To enforce hierarchical priority among modules, a weighted energy cost vector $E_{tmp}$is defined:

$$E_{tmp}(i) = \begin{cases} w_1 E_i, & N_i^{port} = port \wedge N_i^{unit} = unit \\ w_2 E_i, & N_i^{unit} = unit \\ w_3 E_i, & \text{otherwise} \end{cases}$$

with:

$$w_1 < w_2 < w_3$$

The optimization objective is:

$$\min_{\mathbf{m}} \sum_{i=1}^{C_{all}} E_{tmp}(i)\, m_i$$

4. Constraints

4.1 Power Demand Constraint

$$\sum_{i=1}^{C_{all}} P_i\, m_i \ \geq \ P_{EV}$$

This ensures the EV power demand is satisfied.

4.2 Module Availability Constraint

$$0 \leq m_i \leq A_i, \forall i$$

Unavailable modules ($A_i = 0$) cannot be selected.

4.3 Hierarchical Feasibility Constraints

To preserve modularity and reduce inter-port coupling, the algorithm solves **three LPs with progressively relaxed feasible sets**.

Case 1: Same Port and Same Unit

$$A_i^{(1)} = \begin{cases} A_i, & N_i^{port} = port \wedge N_i^{unit} = unit \\ 0, & \text{otherwise} \end{cases}$$

Case 2: Same Unit (Different Ports Allowed)

$$A_i^{(2)} = \begin{cases} A_i, & N_i^{unit} = unit \\ 0, & \text{otherwise} \end{cases}$$

Case 3: All Modules

$$A_i^{(3)} = A_i$$

5. Optimization Problems Solved

At each hierarchical level $k \in \{1,2,3\}$, the following LP is solved:

$$\min_{\mathbf{m}} \quad \sum_{i=1}^{C_{all}} E_{tmp}(i)\, m_i$$

$$\text{s.t.} \quad \sum_{i=1}^{C_{all}} P_i\, m_i \geq P_{EV}$$

$$0 \leq m_i \leq A_i^{(k)}, \forall i$$

If the problem is feasible at level k, the solution is accepted and the algorithm terminates.

6. Optimality and Feasibility Properties

Proposition 1 (Hierarchical Feasibility)

If a feasible solution exists at hierarchy level k, then it is also feasible at any level $k' > k$.

Proof:

Each subsequent level relaxes constraints by expanding the feasible set $A_i^{(k)}$.

Proposition 2 (Priority Optimality)

The algorithm selects the solution with the minimum weighted energy cost among all feasible module subsets satisfying the highest priority level.

Proof:

Since $w_1 < w_2 < w_3$, any solution using lower-priority modules incurs higher cost and is therefore dominated in the LP objective.

7. Relation to OMPC Framework

The proposed algorithm can be interpreted as a static OMPC layer where:

- Each module is a decision agent
- The weighted cost E_{tmp}represents local objective functions
- Hierarchical feasibility mimics constraint tightening and relaxation Central coordination is achieved via LP feasibility rather than explicit Lagrange multipliers

8. Computational Complexity

Each step solves a linear program with:

- C_{all}variables
- $C_{all} + 1$constraints

Worst-case complexity:

$$\mathcal{O}(3 \cdot LP(C_{all}))$$

which is tractable for real-time EV charging applications.

VII. Simulation and Experimental Results

This section presents simulation results for the two case studies described in Section VI. Due to the complexity of multi-unit PEM borrowing, simulations are used to validate the proposed methodology.

A. Simulation Results

1) Case Study 1: Intra-Unit PEM Borrowing

In this scenario, a 50 kW Nissan Leaf is connected to port 1 and a 170 kW Tesla Model 3 is connected to port 2. The nominal voltage is 400 V, the initial battery voltage is 200 V, and the initial state of charge (SoC) for both EVs is 50 % to reduce simulation time.

Based on the reference constant currents (CC) are calculated as:

- Port 1: 62.5 A for the contributing PEMs (PEM11 and PEM21)
- Port 2: 70.8 A for contributing PEMs (PEM12–PEM52) including the borrowed PEM51 from port 1

It shows the response of port 1 PEM currents, powers, SoCs, and charging voltages. PEM11 and PEM21 share the power equally, while PEM31 and PEM41 remain idle. PEM51 follows the charging profile of port 2, demonstrating successful PEM borrowing. The transition from CC to CV mode at 80 % SoC is smooth, confirming the seamless mode-switching capability of the proposed control strategy.

It illustrates port 2 PEM responses. The total current represents the sum of all local PEMs and the borrowed PEM. All contributing PEMs share power equally and remain synchronized, validating proper power distribution among multiple modules.

2) Case Study 2: Inter-Unit PEM Borrowing

In this scenario, a 50 kW Nissan Leaf is connected to port 1, and a 250 kW, 400 V Tesla Model 3 LARP is connected to port 2 of another charger. To meet the high power requirement, port 2 borrows three PEMs from its own port 1 and one PEM from port 1 of a neighboring charging unit, resulting in a total of nine PEMs. The reference CC for each PEM is 69.4 A. It shows the response of port 1 in the first charging unit, which lends one module to the second port of the same unit and another module to the second charging unit. The fourth module follows the borrowed charging profile, while the first and second modules continue following the local controller. Module 5 adopts the profile from the neighboring unit.

These results confirm that the proposed PEM borrowing strategy enables flexible inter-port and inter-unit power sharing without degrading the performance of the original port or increasing charging time. The simulation demonstrates that all PEMs are effectively utilized, and the charging ports can deliver the requested power to EVs while maintaining safe voltage and current profiles.

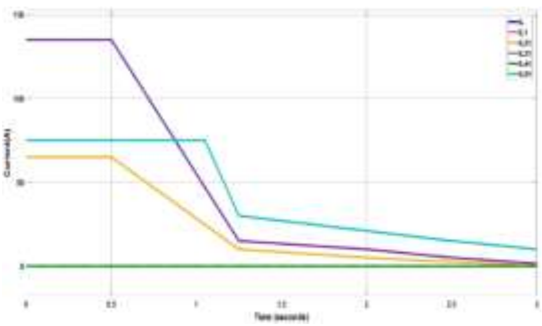

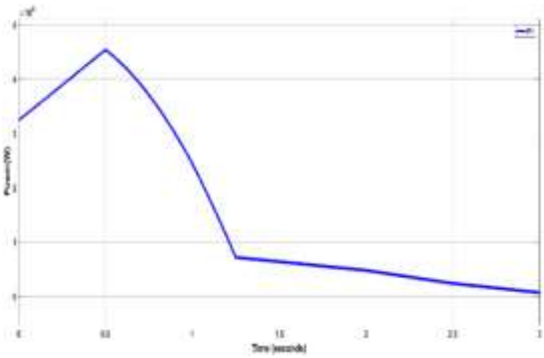

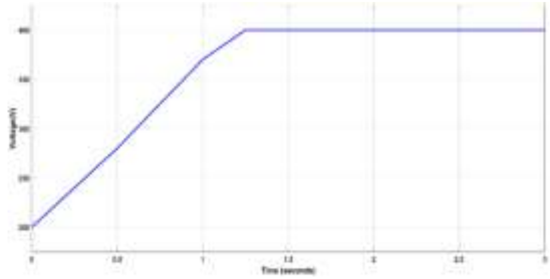

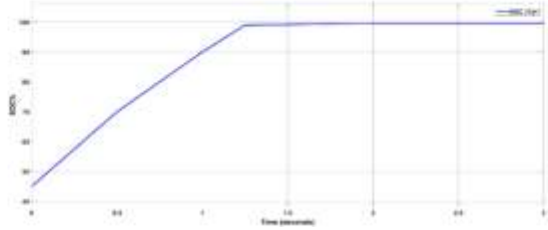

Fig. 6. Case 1: currents, power, SoC, and charging voltage. (a) Port 1.

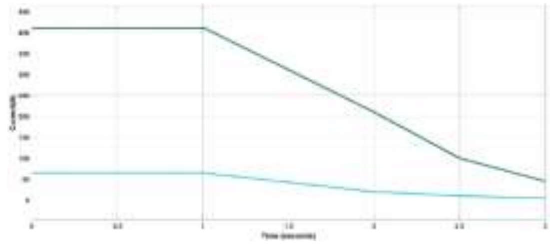

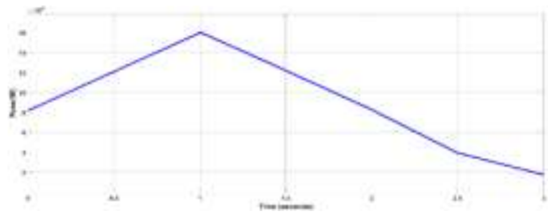

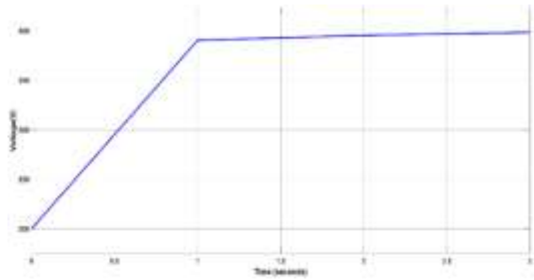

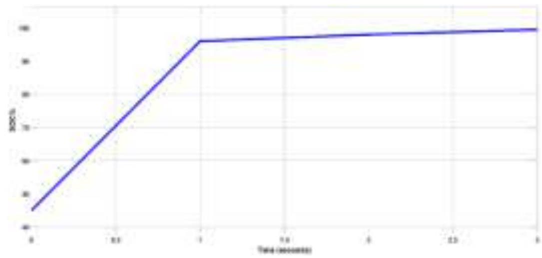

Fig. 7. Case 1: currents, power, SoC, and charging voltage Port 2.

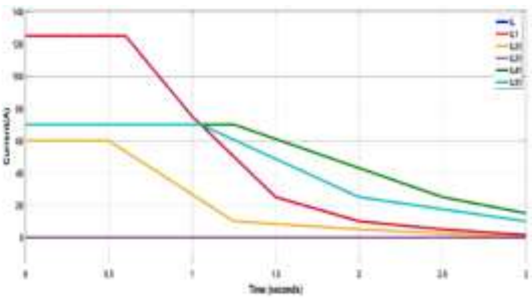

Fig. 8. Case2: The response of charging unit 1 port1.

CONCLUSION

This paper presented a Hierarchical Optimization-Based Optimal Modular Power Coordination (OMPC) algorithm for multimodule, multiport Fast Electric Vehicle Chargers (FEVCs). The proposed approach integrates a mixed-integer optimization layer for strategic module selection and a real-time convex optimization layer for power-sharing among modules, while introducing the novel concept of PEM borrowing for flexible inter-port and inter-unit power allocation.

Simulation results for two case studies demonstrated that:

1. The proposed OMPC algorithm enables seamless sharing of PEMs between ports, ensuring that connected EVs receive their nominal charging power.
2. Inter-unit PEM borrowing effectively expands available charging capacity, allowing high-power EVs to charge simultaneously with lower-power EVs without increasing overall charging time.
3. The hierarchical control methodology ensures smooth CC–CV transitions, accurate voltage and current regulation, and balanced utilization of PEMs.

Overall, the OMPC algorithm enhances the charging flexibility, module utilization, and scalability of multimodule FEVC systems, making it a promising solution for next-generation fast-charging infrastructure. Future work includes experimental validation with larger-scale chargers and integration with smart-grid energy management to optimize system-level performance under dynamic grid conditions.

REFERENCES

[1] F. Un-Noor, S. Padmanaban, L. Mihet-Popa, M. N. Mollah, and E. Hossain, "A comprehensive study of key electric vehicle (EV) components, technologies, challenges, impacts, and future direction of development," Energies, vol. 10, no. 8, pp. 1217, 2017.

[2] F. Blaabjerg, H. Wang, I. Vernica, B. Liu, and P. Davari, "Reliability of power electronic systems for EV/HEV applications," Proc. IEEE, vol. 109, no. 6, pp. 1060–1076, Jun. 2021.

[3] A New Configuration of Nine Level Switched Capacitor Boost Inverter of Single DC Source with Reduced Component Count. (2025). *International Research Journal on Advanced Engineering Hub (IRJAEH)*, *3*(10), 3919-3924.

[4] Srinivasa Kalyan Immadi. (2025). Harnessing Artificial Intelligence In Oracle Hcm: Revolutionising Workforce Management With Automation And Predictive Analytics. International Journal of Data Science and IoT Management System, 4(4), 7–13. https://doi.org/10.64751/ijdim.2025.v4.n4.pp7-13.

[5] I. S. Bayram, U. Zafar, and S. Bayhan, "Could petrol stations play a key role in transportation electrification? A GIS-based coverage maximization of fast EV chargers in urban environment," IEEE Access, vol.

10, pp. 17318–17329, 2022, doi: 10.1109/ACCESS.2022.3149758.

[6] Explainable AI Framework for Policy-Compliant Anomaly Detection in Data Pipelines. (2025). Inaternational Journal of Communication Networks and Information Security, 16(4). https://doi.org/10.48047/ijcnis.16.4.2111.

[7] Bhagwat, V. B. (2025). Simplifying Payroll Balance Conversions in Payroll Systems Implementation through the Use of Generative AI.

[8] Todupunuri, A. (2023). The Role of Artificial Intelligence in Enhancing Cybersecurity Measures in Online Banking Using AI. International Journal of Enhanced Research in Management & Computer Applications, 12(01), 103–108. https://doi.org/10.55948/ijermca.2023.01015.

[9] Suhasnadh Reddy Veluru, Sai Teja Erukude, and Viswa Chaitanya Marella. 2025. Multimodal Detection of Fake Reviews using BERT and ResNet-50. In 2025 4th International Conference on Innovative Mechanisms for Industry Applications (ICIMIA). IEEE, 877–882.

[10] A. Sharida, S. Bayhan, and H. Abu-Rub, “Fault-tolerant self-tuning control for three-phase three-level t-type rectifier,” IEEE Trans. Power Electron., vol. 38, no. 6, pp. 7049–7058, Jun. 2023.

[11] K.Meenendranath Reddy, Dr. P.Sankar Babu, “OFF-Board Electrical Vehicle Battery Charger Using PV Array”, in Journal of Engineering Sciences, Vol 14 Issue 04, April 2023.

[12] S. Tan, et al., “Hierarchical optimization-based energy management for multiport EV chargers,” IEEE Trans. Ind. Electron., vol. 67, no. 8, pp. 6622–6633, Aug. 2020.

[13] Gaddam, S. (2025). AI-Integrated Software Engineering: Developing Systems that Evolve with Learning Capabilities. Journal of Information Systems Engineering and Management, 10(63s)..

[14] P. Naga Sai Charan, & K. Meenendranath Reddy. (2023). An Analysis of Multilevel Converter for Faster Current Control in a DC Microgrid with Extremely Low- Impedance Interconnections. *Journal of Image Processing and Intelligent Remote Sensing*, *3*(01), 18–29.

[15] J. A. Ferreira, et al., “Power sharing in multiport EV chargers: analysis and implementation,” IEEE Access, vol. 8, pp. 144567–144578, 2020.